МАТЕРІАЛИ ДЛЯ СЕНСОРІВ

SENSOR MATERIALS

PACS77.55.hf, 33.60.+q, 79.60.-i, 82.80.Pv, 68.37.Hk, 81.15.Cd, 68.37.-d, 78.20.-e, 78.66.-w
DOI: https://doi.org/10.18524/1815–7459.2024.1.300942

MORPHOLOGICAL, OPTICAL PROPERTIES AND ELECTRONIC STRUCTURE OF ZnO THIN FILMS DOPED WITH ALUMINUM

V. V. Zaika[1], N. K. Shvachko[2]

Kurdyumov Institute for Metal Physics of the National Academy of Sciences of Ukraine, 36, Academician Vernadsky Blvd, 03142 Kyiv, Ukraine
[1] +38(068)774–79–32, zaikavladimir228@gmail.com
[2] +38(095)550–48–99, nazarii1999@gmail.com

MORPHOLOGICAL, OPTICAL PROPERTIES AND ELECTRONIC STRUCTURE OF ZnO THIN FILMS DOPED WITH ALUMINUM

V. V. Zaika, N. K. Shvachko

Abstract. This paper presents the results of investigation of aluminum-doped zinc oxide thin films obtained by radio-frequency magnetron deposition on a glass substrate. It was shown by energy dispersion X-ray spectroscopy that the average aluminum content in the thin films was 0.2–0.8 at.%. An increase in the average grain size with increasing aluminum concentration was shown, and column-like growth of the films was established using microscopic images. Investigation of the electronic structure showed a redistribution of intensity in the O 1*s* spectrum with aluminum doping. The valence band spectra were also obtained, and theoretical calculations were performed within the framework of density functional theory to better understanding the results. Using a spectrophotometer, the transparency of the films obtained after aluminum doping was shown to increase. With the help of the Tauc method, the band gap was determined to be 3.41 eV, while DFT calculations showed a band gap of 1.25 eV.

Keywords: nanostructured thin films, RF magnetron sputtering, doped, electronic structure

МОРФОЛОГІЧНІ, ОПТИЧНІ ВЛАСТИВОСТІ ТА ЕЛЕКТРОННА БУДОВА ТОНКИХ ПЛІВОК ZnO ДОПОВАНИХ АЛЮМІНІЄМ

В. В. Заіка, Н. К. Швачко

Анотація. В даній роботі представлені результати досліджень тонких плівок окисі цинку допованих алюмінієм, які отримані методом радіочастотного магнетронного нанесення на скляній підкладці. За допомогою енергодисперсійного рентгенівського аналізу показано, що середній вміст алюмінію в тонких плівках становив 0.2–0.8 at.%. Було показано ріст середнього розміру нанозерен при збільшенні концентрації алюмінію, а також за допомогою мікроскопічних знімків поперечного перерізу було встановлено стовпчастий ріст плівок. Дослідження електронної будови показали перерозподіл інтенсивності в O *1s* спектрі після допування алюмінієм. Також були отримані спектри валентної зони, та проведені теоретичні розрахунки в рамках теорії функціоналу густини для кращої інтерпретації отриманих результатів. Методом Таука була визначена ширина забороненої зони яка становила 3.41еВ, тоді як в рамках DFT розрахунків заборонена зона становила 1.25 еВ.

Ключові слова: наноструктуровані тонкі плівки, ВЧ магнетронне розпилення, легування, електронна структура

Introduction

Zinc oxide (ZnO) is a well-known material due to its wide range of applications, that include varistors, additives for paints, cement, and rubber, thin-film transistors, visible-blind photodetectors, gas sensors, transparent conductive oxides, and other devices. These diverse applications are due to a set of unique properties of ZnO. These include a straight, wide band gap, a high exciton binding energy, good transparency in the visible and infrared spectrum, low cost of ZnO, and environmental safety.

ZnO thin films can be obtained by various physical and chemical methods of deposition, in particular, sol-gel, radiofrequency magnetron deposition, and molecular beam epitaxy [1–3]. Among the above methods, radiofrequency magnetron deposition stands out due to the simplicity of the process, homogeneity of the films obtained, and their elemental purity. Additionally, the synthesis can be economically optimized by eliminating the process of baking of the ceramic target, which requires high temperatures and, therefore, significant energy consumption. One way to realize this is the production of thin films using magnetron deposition of a pressed powder target.

Despite a considerable number of studies of aluminum-doped ZnO films [4–6], the effect of aluminum on morphological properties and electronic structure is still not sufficiently covered.

Based on this, the objectives of this work are:

- Synthesize ZnO thin films as well as ZnO films doped with aluminum using pressed powder targets.
- Study their morphological and optical properties and electronic structure.
- Determine the chemical composition of the obtained films.
- Determine the effect of aluminum on the morphological and optical properties and establish its influence on the electronic structure.

Methods of synthesis and characterization

ZnO thin films were deposited by radiofrequency magnetron deposition using a high-purity target of pressed ZnO (99.9%) powder with a diameter of 4.0 cm (12.57 cm^2). Aluminum doping was performed by mixing ZnO (99.9%) and Al_2O_3 (>98%) powders in a weight ratio of 99:1, 98:2, 97:3 for ZnO1%, ZnO2%, and ZnO3% samples, respectively, and then mixing

the powders for an hour. A microscopy glass slide (1x1 cm^2) was used as a substrate. It was cleaned beforehand with acetone and isopropyl alcohol in an ultrasonic bath for 20 minutes and rinsed with deionized water. After that, the glass was transported to a vacuum chamber and placed above the ZnO target at a distance of 4.5 cm. A pre-vacuum and a diffusion pump equipped with a nitrogen trap were used to obtain a high vacuum of $5.0x10^{-5}$ Pa. Argon (99.9%) was used to produce the plasma. The pressure inside the chamber during deposition was $1.0x10^{-2}$ Pa. The films were deposited at a magnetron power of 100 W. The target was pre-deposited for 10 minutes to clean its surface, and then the films were deposited during 60 minutes and under the identical synthesis conditions.

The morphological analysis of the surface after the growth of ZnO thin films was performed by scanning electron microscopy (SEM) using a Tescan Mira 3 microscope. This microscope is equipped with an EDX detector, which allows to perform the chemical analysis.

The X-ray photoelectron spectroscopy (XPS) spectra of the core levels of the samples were obtained on a JEOL XPS2400 X-ray spectrometer. The operating pressure during the experiment was no more than $1.0x10^{-7}$ Pa. The radiation of the magnesium anode with the energy of the Mg Kα line of 1253.6 eV was used. The energy resolution was 0.1 eV. The charge correction was performed by using the C1*s* spectral line centroid with an energy of 284.0 eV as a reference point.

We used the Quantum Espresso Simulation Package [7] for all density functional theory (DFT) calculations with projector augmented wave (PAW) pseudopotentials [8]. We used a plane wave cut-off energy of 816 eV and a 9×9×3 Gamma-centered k-point grid for structural optimizations and a 32×32×16 Gamma-centered k-point grid for density of states calculations. All calculations are done using the generalized gradient approximation (GGA) based exchange-correlation functional PBEsol [9], with a Hubbard-U of 7.5 eV (as per [10]) applied to the Zn-d states as implemented with the Dudarev[11] approach unless otherwise stated.

Results and discussion

The morphological features of the thin films were studied by SEM (Fig. 1). The morphology of the ZnO film consists of densely packed grains of almost spherical shape. The ZnO1% film also consists of almost spherical grains, but the coalescence of some grains can be observed, resulting in the formation of elongated particles with a more elliptical shape. It is easy to notice a significant increase in nanograins size for the ZnO2% film due to a higher degree of coalescence. However, for the ZnO3% film, the number of large grains as well as their size decreased. It can be observed that a small number of petal-like grains appear (Fig. 1 d), which may indicate a change in the growth kinetics. It is worth noting the developed nanoscale structure of the surface of obtained films despite their relative smoothness. Thus, it can be assumed that the addition of aluminum leads to a decrease in the surface area, which can alter both the adsorption properties of the film and the surface energy.

In order to estimate the thickness of the samples, the surfaces of the films were locally destroyed by scratching the surface with a scalpel (Fig. 2). The thicknesses of the films were 270.0, 292.0, 410.0, 349.0 nm for ZnO, ZnO1%, ZnO2%, and ZnO3% samples, respectively. The increase in the growth rate may be due to the greater number of electrons in an Al^{3+} ion compared to Zn^{2+}, which affects the number of nucleation centers in the initial stages of growth. From the cross-sectional image, the column-like structure of the films can be established. The explanation for this phenomenon is described in [12]. It consists in the selection of crystals with the fastest growth rates perpendicular to the substrate, which is governed by the principle of "survival of the fastest". This growth is also characterized in the structural zone model proposed by J. V. Sanders [13], which states that the temperature range 0.1 < synthesis temperature/melting temperature < 0.3 corresponds to the conditions when surface diffusion becomes noticeable and as a result, a column-like structure with impermeable boundaries is formed.

Given that the mean free path of characteristic X-rays is much longer than the

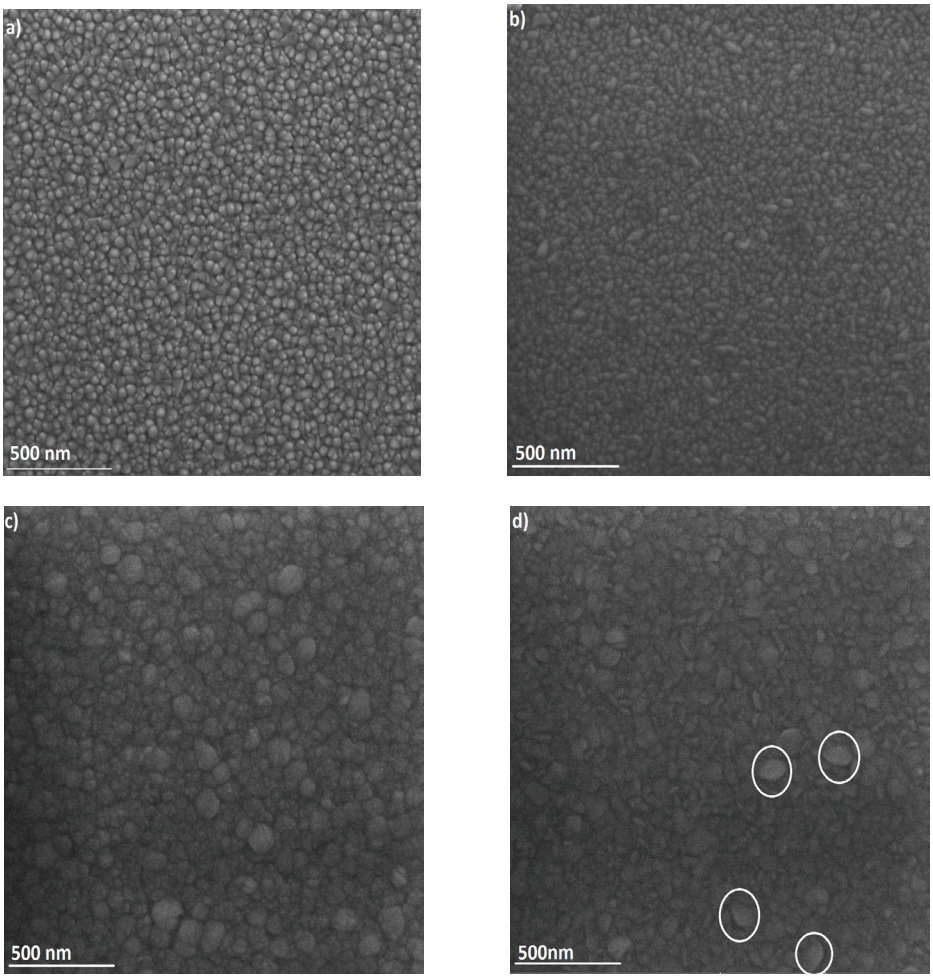

Fig. 1. SEM images of samples. a) ZnO b) ZnO1% c) ZnO2% d) ZnO3%.

thickness of the films obtained, in order to perform the EDX analysis the films were scraped off with a scalpel and transported onto a conductive carbon tape. The EDX analysis revealed the presence of 4 elements, namely Zn, O, Al and C (Fig. 3). Taking into account the chemical composition of the tape, carbon was excluded from the EDX analysis. The results of EDX analysis revealed successful doping of the films with aluminum, but its concentration was lower than expected. A larger amount of zinc than oxygen was observed, which is typical for films obtained by radio-frequency magnetron deposition using argon. Also, the non-stoichiometric Zn/O ratio may indicate a significant amount of oxygen vacancies or interstitial zinc atoms. Given the low migration energy barrier for interstitial zinc of 0.57 eV [14], the oxygen deficiency can be explained by a large number of oxygen vacancies.

To clarify the features of the electronic structure, XPS studies were performed (Fig. 4). The energy of Zn $2p_{3/2}$ is 1021.4 eV, and Zn $2p_{1/2}$ is 1044.5 eV. The spin-orbit splitting for Zn, $2p_{3/2}$–$2p_{1/2}$, amounts to 23.1 eV, which is characteristic of ZnO. The peaks with energies of 1036.0 and 1012.9 appear due to satellites from Mg K $\alpha_{3,4}$ [15], which are located in the direction of lower binding energies at a distance of 8.5 eV.

Changes in the O 1*s* spectrum after the doping of ZnO with aluminum were attested. In the literature, the decomposition of O 1*s* peak into 3 components is accepted. The low-energy peak is attributed to O^{2-} ions in the ZnO matrix with predominantly Zn-O (or Zn substituted by

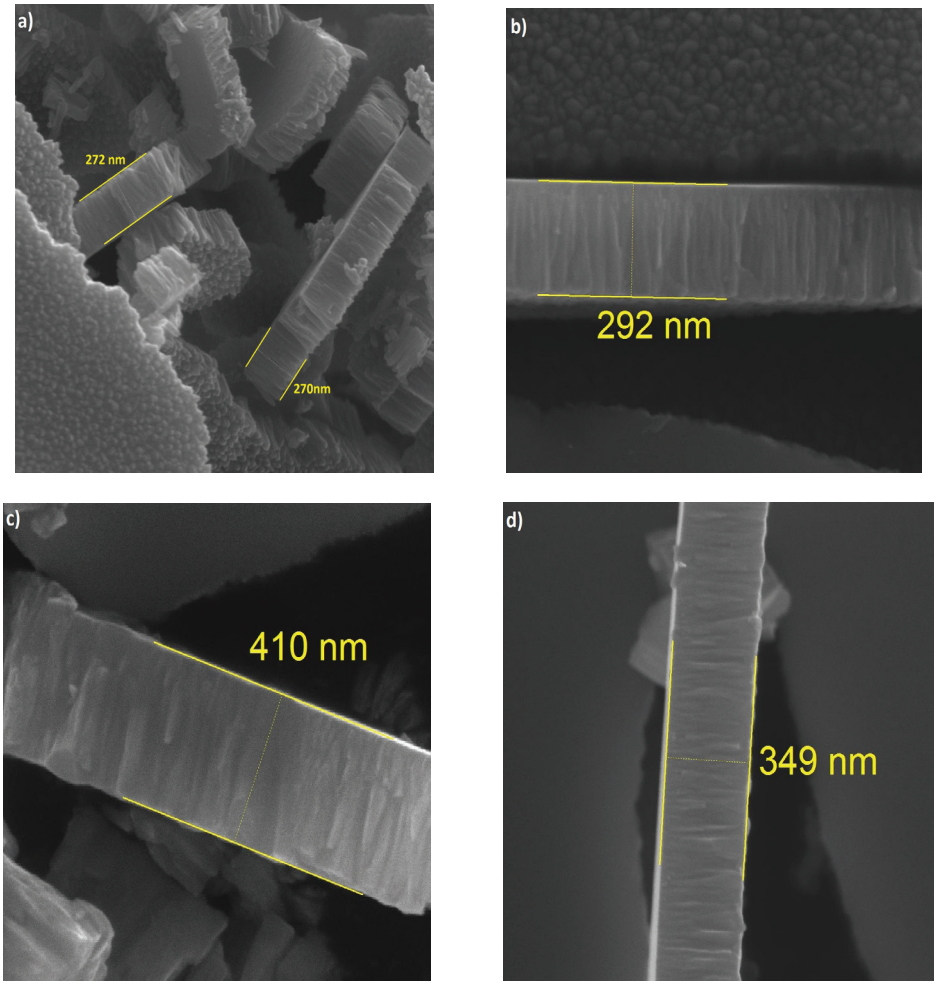

Fig. 2. Estimation of film thickness by SEM. a) ZnO b) ZnO1% c) ZnO3% d) ZnO3%.

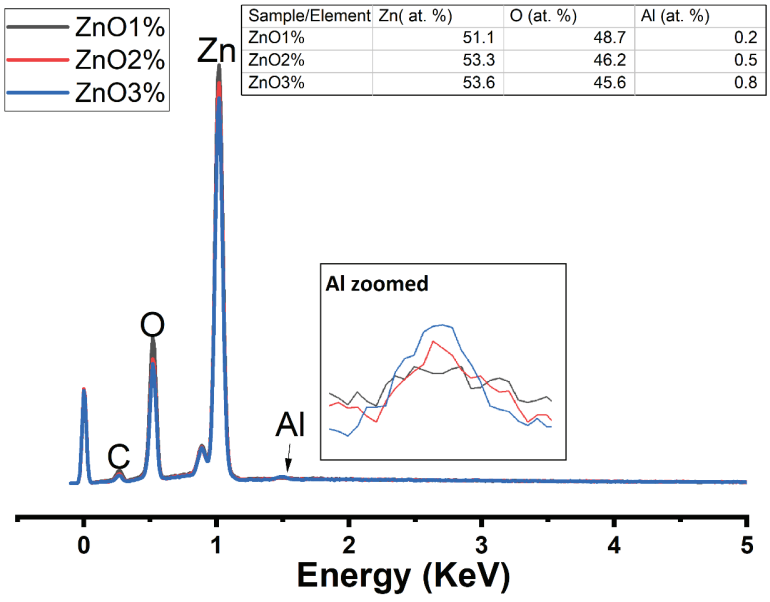

Sample/Element	Zn(at. %)	O (at. %)	Al (at. %)
ZnO1%	51.1	48.7	0.2
ZnO2%	53.3	46.2	0.5
ZnO3%	53.6	45.6	0.8

Fig. 3. EDX analysis of ZnO1%, ZnO2%, ZnO3%.

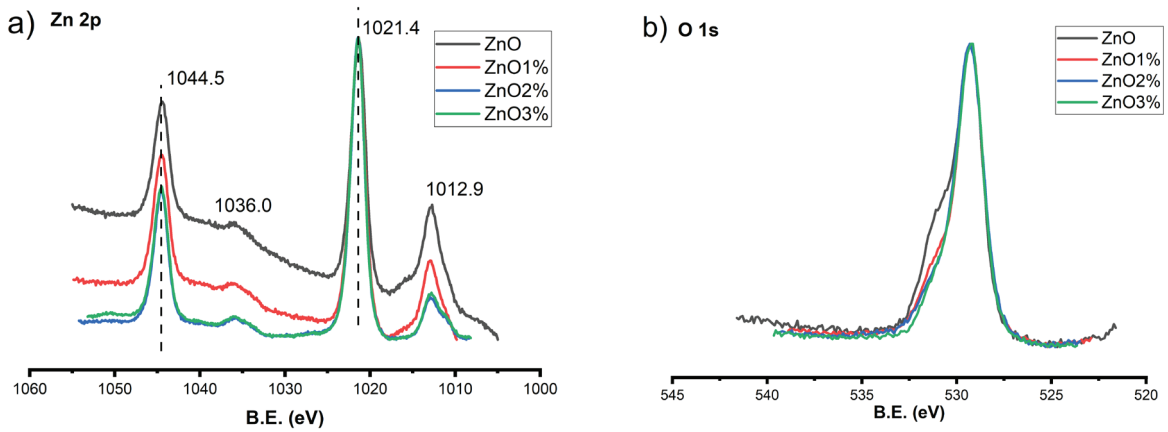

Fig. 4. XPS spectra of a) Zn 2*p*; b) O 1*s*.

Al) ionic bonds [16], while middle peak belongs to O^{2-} ions in oxygen-deficient regions [17], and the high-energy peak stems from the adsorbed or chemically adsorbed forms of oxygen, namely CO, H_2O, or surface hydroxyl groups [18]. Thus, the decrease in the intensity of the higher-energy components of the O 1*s* spectrum can be explained by a decrease in the number of adsorbed oxygen species on the surface. This statement also correlates with a decrease in oxygen in the EDX spectra and an increase in the size of nanograins on the surface, which ultimately reduces the total surface area.

Figure 5 (a) shows the valence band of ZnO and aluminum-doped ZnO thin films. DFT calculations of electronic structure of ZnO were also performed (Fig. 5b) for a better interpretation of the results. Comparing the experimental data with the calculated data, one can notice a good agreement of the total density of states (DOS) between experiment and theory. Thus, it is easy to see that the top of the valence band is almost entirely composed of 2*p* oxygen states and the bottom of the valence band is composed of 3*d* zinc states. Given the almost identical energy of the states near the top of the valence band of Zn 4*s* and O 2*p, we* can assume their partial hybridization. After the addition of aluminum, a significant decrease in the electron density in the range from 2.0 to 5.0 eV is observed, which to the best of our knowledge is the first time it has been reported. Within the framework of DFT calculations, it was determined that ZnO has a direct band gap at the Γ point of the Brillouin zone with a width of 1.25 eV.

For many applications, transparency in the visible range is an extremely important parameter. Relatively high transparency was observed for all the films obtained, as well as a clear onset of the absorption edge at 370 nm. The transparency of all films was > 75% in the entire visible and near-infrared range (Fig. 6a). Transparency fluctuations are associated with interference effects and confirm the smooth surface of the films obtained. Using the Tauc plot [20], the band gap was determined to be 3.41 eV (Fig. 6b). An observed increase in the band gap after aluminum doping might occur due to the Moss-Berstein effect [21]. For example, in [22], an increase in the band gap from 3.33 eV to 3.36 eV was observed after aluminum doping, but the resolution of our spectrophotometer does not allow us to determine such small changes.

Conclusions

In the present work, aluminum-doped ZnO thin films were successfully synthesized using radio-frequency magnetron deposition with using a powder target. Upon doping with aluminum, an increase in the average nanograin size is observed due to increased coalescence, which can affect the adsorption properties and surface energy of the thin films. Using SEM cross-sectional images of thin films the columnar growth of the films was

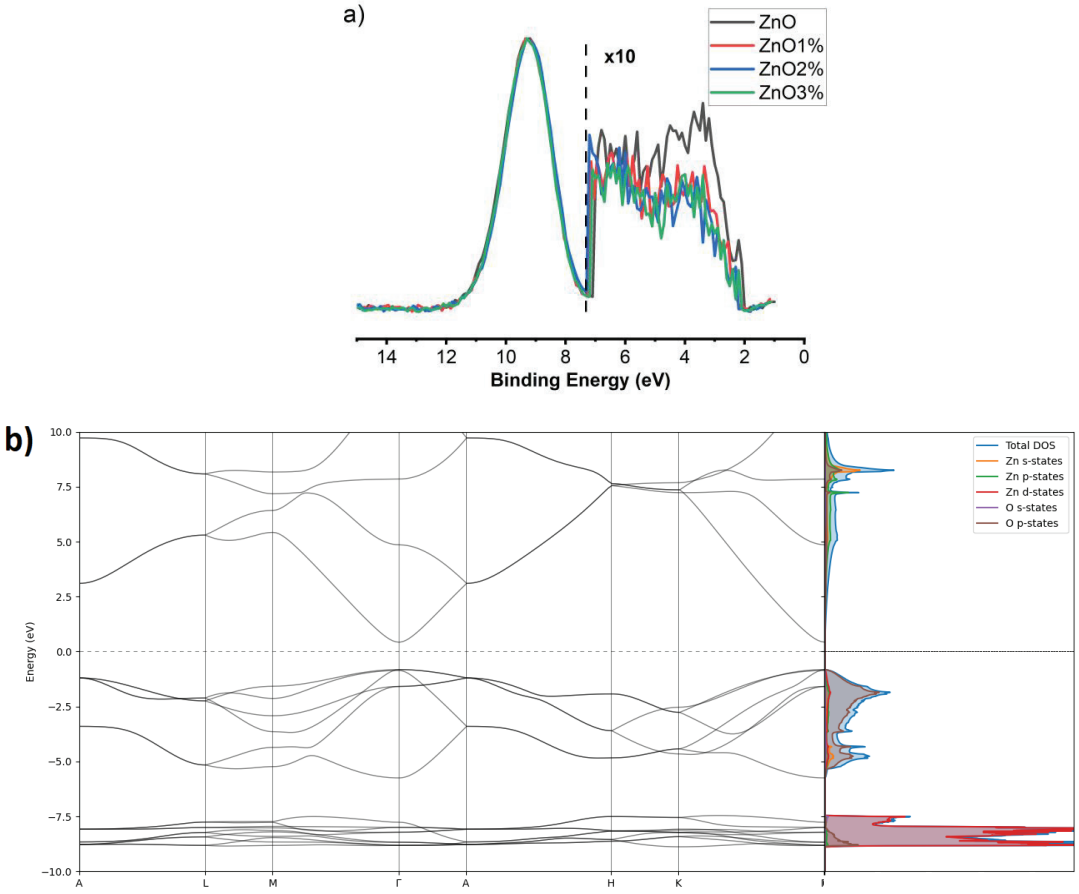

Fig. 5. (a) XPS spectra of the valence band. Taking into account the small photoionization cross section under Mg Kα irradiation for O *2p* = 0.0193 [19], part of the spectrum was multiplied by 10. b) ZnO band structure and the density of states obtained by DFT calculations.

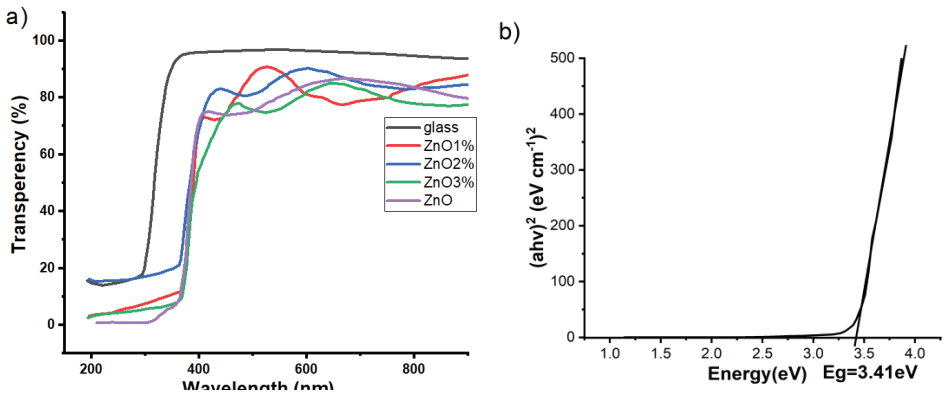

Fig. 6. (a) Transmission spectra of thin films. b) Determination of the band gap of ZnO by the Tauc plot.

observed, which is explained by the selectivity of crystals with the fastest growth rates perpendicular to the substrate. The oxygen deficiency in the obtained films was found to be due to a large number of oxygen vacancies. The decrease of adsorbed oxygen species was established from the redistribution of O 1*s* intensity. The top of the valence band is predominantly composed of 2*p*

oxygen states, while the bottom is characterized by the presence of 3*d* zinc states. To the best of our knowledge, a decrease in the density of states in the energy range from 2.0 to 5.0 eV after aluminum doping is observed for the first time. The obtained films have relatively good transparency of more than 75% in the visible and near-infrared spectral region. The band gap determined by the Tauc plot was 3.41 eV, and the one obtained in DFT calculations was 1.25 eV.

References

[1]. L. Znaidi. Sol–gel-deposited ZnO thin films: A review // Mater. Sci. Eng. B-Adv., 174(1–3), pp. 18–30 (2010).

[2]. M. Opel, S. Geprägs, M. Althammer, T. Brenninger, R. Gross. Laser molecular beam epitaxy of ZnO thin films and heterostructures // J. Phys. D. Appl. Phys., 47(3), 034002 (2013).

[3]. P. -F. Yang, H. -C. Wen, S. -R. Jian, Y. -S. Lai, S. Wu & R. -S. Chen. Characteristics of ZnO thin films prepared by radio frequency magnetron sputtering //Microelectron. Reliab., 48(3), pp. 389–394 (2008).

[4]. Z. Zhang, C. Bao, W. Yao, S. Ma, L. Zhang & S. Hou. Influence of deposition temperature on the crystallinity of Al-doped ZnO thin films at glass substrates prepared by RF magnetron sputtering method // Superlattice. Mictost., 49(6), pp. 644–653 (2011).

[5]. D. K. Kim & H. B. Kim. Room temperature deposition of Al-doped ZnO thin films on glass by RF magnetron sputtering under different Ar gas pressure // J. Alloy. Compd., 509(2), pp. 421–425 (2011).

[6]. R. S. Tondare, B. W. Shivaraj, H. N. Narasimhamurthy, M. Krishna & T. K. Subramanyam. Effect of deposition time on structural, electrical and optical properties of Aluminium doped ZnO thin films by RF magnetron sputtering // Mater. Today-proc., 5(1), pp. 2710–2715 (2018).

[7]. P. Giannozzi, S. Baroni, N. Bonini, M. Calandra, R. Car, C. Cavazzoni, D. Ceresoli, G. L. Chiarotti, M. Cococcioni, I. Dabo, A. Dal Corso, S. Fabris, G. Fratesi, S. de Gironcoli, R. Gebauer, U. Gerstmann, C. Gougoussis, A. Kokalj, M. Lazzeri, L. Martin-Samos, N. Marzari, F. Mauri, R. Mazzarello, S. Paolini, A. Pasquarello, L. Paulatto, C. Sbraccia, S. Scandolo, G. Sclauzero, A. P. Seitsonen, A. Smogunov, P. Umari, R. M. Wentzcovitch. QUANTUM ESPRESSO: a modular and open-source software project for quantum simulations of materials // Condens. Matter. Phys., 21, 395502 (2009).

[8]. G. Kresse and D. Joubert. Kresse, G., & Joubert, D. (1999). From ultrasoft pseudopotentials to the projector augmented-wave method // Phys. Rev. B., 59(3), pp. 1758–1775 (1999).

[9]. J. P. Perdew, A. Ruzsinszky, G. I. Csonka, O. A. Vydrov, G. E. Scuseria, L. A. Constantin, X. Zhou, and K. Burke // Phys. Rev. Lett., 102, 039902 (2009).

[10]. P. Erhart, K. Albe & A. Klein. First-principles study of intrinsic point defects in ZnO: Role of band structure, volume relaxation, and finite-size effects // Phys. Rev. B., 73(20), 205203 (2006).

[11]. S. L. Dudarev, G. A. Botton, S. Y. Savrasov, C. J. Humphreys, and A. P. Sutton, Electron-energy-loss spectra and the structural stability of nickel oxide: An LSDA+U study// Phys. Rev. B., 57, 1505 (1998).

[12]. A. van der Drift. Evolutionary selection, a principle governing growth orientation in vapour-deposited layers// Philips Res. Repts., 22, 267–288. (1967).

[13]. J. V. Sanders. “Structure of evaporated metal films” in Chemisorption and Reactions on Metal Films //Academic Press, New York, pp 1–38 (1971).

[14]. A. Janotti C. G. Van de Walle. Native point defects in ZnO // Phys Revi B., 76(16) 165202 (2007).

[15]. M. O. Krause, J. G. Ferreira. K X-ray emission spectra of Mg and Al // J. Phys. B-At. Mol. Opt., 8(12), pp. 2007–2014 (1975).

[16]. R. Al-Gaashani, S. Radiman, A. R. Daud, N. Tabet, Y. Al-Douri, XPS and optical studies of different morphologies of ZnO nanostructures prepared by microwave methods // Ceram. Int., 39(3), pp. 2283–2292 (2013).

[17]. D. K. Kim and H. B. Kim, Room temperature deposition of Al-doped ZnO thin films on glass by RF magnetron sputtering under different Ar gas pressure // J. Alloy. Compd., 509(2), pp. 421–425 (2011).

[18]. V. P. Singh and Ch. Rath, Passivation of native defects of ZnO by doping Mg detected through various spectroscopic techniques // Rsc. Adv., 5(55), pp. 44390–44397 (2015).

[19]. N. Ikeo, Y. Iijima, N. Niimura et al., Handbook of X-ray photoelectron spectroscopy. JEOL Ltd 216 s. (1991).

[20]. J. Tauc, Optical properties and electronic structure of amorphous Ge and Si // Mater. Res. Bull., 3(1), pp. 37–46 (1968).

[21]. T. S. Moss. The Interpretation of the Properties of Indium Antimonide// Proc. Phys. Soc., 67(10), 775–782 (1954).

[22]. K. Lovchinov, K. Nichev, O. Angelov, M. Sendova-Vassileva, V. Mikli, D. Dimova-Malinovska. Structural, optical and electrical properties of V doped ZnO thin films deposited by r.f. magnetron sputtering // J. of Phys.: Conference Series, 253, 012030 (2010).

Стаття надійшла до редакції 11.03.2024 р.

PACS77.55.hf, 33.60.+q, 79.60.-i, 82.80.Pv, 68.37.Hk, 81.15.Cd, 68.37.-d, 78.20.-e, 78.66.-w
DOI: https://doi.org/10.18524/1815–7459.2024.1.300942

MORPHOLOGICAL, OPTICAL PROPERTIES AND ELECTRONIC STRUCTURE OF ZnO THIN FILMS DOPED WITH ALUMINUM

V. V. Zaika[1], N. K. Shvachko[2]

Kurdyumov Institute for Metal Physics of the National Academy of Sciences of Ukraine,
36, Academician Vernadsky Blvd, 03142 Kyiv, Ukraine
[1] +38(068)774–79–32, zaikavladimir228@gmail.com
[2] +38(095)550–48–99, nazarii1999@gmail.com

Summary

The aim of the work was to determine the effect of aluminium on the morphological and optical properties of ZnO thin films, as well as to clarify its influence on the electronic structure. To achieve these goals, scanning electron microscopy, energy-dispersive X-ray spectroscopy, X-ray photoelectron spectroscopy, and spectrophotometric methods were chosen. It was found that the average size of nanograins on the surface increased after aluminium doping, and that the films demonstrated columnar growth, as cross-sectional images show. An increase in the growth rate of the films after aluminium doping was also observed. Using energy-dispersive X-ray spectroscopy, it was found that the films are characterised by the presence of oxygen deficiency, which is explained by a large number of oxygen vacancies. It is reasonable to assume a decrease in the amount of adsorbed oxygen species on the surface of the films after aluminium doping, based on the redistribution of the O *1s* line intensity. For a better explanation of the photoelectron spectra of the occupied part of the valence band, density functional theory (DFT) calculations were performed. It is shown that the ceiling of the valence band is almost entirely composed of *2p* oxygen electrons, and the bottom of the valence band is composed of *3d* zinc electrons. Also, taking into account the same energy of O *2p* and Zn *4s* electrons, we can assume their partial hybridization. Furthermore, after the addition of aluminium, a decrease in the intensity in energy range from 2.0 to 5.0 eV within the valence band was observed, to our best knowledge, for the first time. The transparency of all the films obtained in the visible spectral region was > 75%. Also, using the Tauc method, the band gap was found to be 3.41 eV. Within the framework of the DFT, the value of the band gap was 1.25 eV, which is explained by the well-known fact that the band gap decreases in DFT calculations.

Keywords: nanostructured thin films, RF magnetron sputtering, doping, electronic structure

PACS77.55.hf, 33.60.+q, 79.60.-i, 82.80.Pv, 68.37.Hk, 81.15.Cd, 68.37.-d, 78.20.-e, 78.66.-w
DOI: https://doi.org/10.18524/1815–7459.2024.1.300942

МОРФОЛОГІЧНІ, ОПТИЧНІ ВЛАСТИВОСТІ ТА ЕЛЕКТРОННА БУДОВА ТОНКИХ ПЛІВОК ZnO, ДОПОВАНИХ АЛЮМІНІЄМ

В. В. Заіка[1], Н. К. Швачко[2]

Інститут металофізики ім. Г. В. Курдюмова НАН України,
бульв. Академіка Вернадського, 36, 03142 Київ, Україна
[1] +38(068)774–79–32, zaikavladimir228@gmail.com
[2] +38(095)550–48–99, nazarii1999@gmail.com

Реферат

Мета роботи полягала у визначенні впливу алюмінію на морфологічні, оптичні властивості тонких плівок ZnO, а також з'ясуванні його впливу на електрону будову. Для досягнення поставлених цілей були обрані методі сканувальної електронної мікроскопії, рентгенівської енергодисперсійної спектроскопії, рентгенівської фотоелектронної спектроскопії та спектрофотометричні методи досліджень. Було виявлено, що після допування алюмінієм збільшується середній розмір нанозерен на поверхні, а також зі знімків поперечного перерізу плівок встановлено їх стовпчастий ріст. Також спостерігалося збільшення швидкості росту плівок після допування алюмінієм. За допомогою рентгенівської енергодисперсійної спектроскопії було з'ясовано, що отриманим плівкам притаманний дефіцит кисню, який пояснюється великою кількістю кисневих вакансій. Можна припустити зменшення кількості адсорбованих видів кисню на поверхні плівок після допування алюмінієм, виходячи з перерозподілу інтенсивності лінії O *1s*. Для кращої інтерпретації фотоелектронних спектрів зайнятої смуги валентної зони були проведені розрахунки в рамках теорії функціоналу густини (ТФГ). Показано, що стеля валентної смуги майже повністю складається з *2p* електронів кисню, а дно валентної зони – з *3d* електронів цинку. Також, враховуючи однакову енергію електронів O *2p* та Zn *4s,* можна припустити їх часткову гібридизацію. Крім того, після допування алюмінієм спостерігається зменшення інтенсивності у валентній зоні з 2.0 до 5.0 еВ, що, на нашу думку, спостерігається вперше. Прозорість усіх отриманих плівок у видимій області спектру була > 75%. Також, методом Таука була знайдена ширина забороненої зони зі значенням 3.41еВ. В рамках теорії ТФГ значення забороненої зони становило 1.25еВ, що пояснюється загальновідомим фактом зменшення значення забороненої зони в теоретичних розрахунках.

Ключові слова: наноструктуровані тонкі плівки, ВЧ магнетронне розпилення, легування, електронна структура